J Fail. Anal. and Preven. (2008) 8:41–47
DOI 10.1007/s11668-007-9106-5

Damage and Residual Life Assessment of Bends for X20CrMoV12.1 Main Steam Pipe after Long-Term Service

Zheng-Fei Hu · Zheng-Guo Yang · Guo-Qiu He · Cheng-Shu Chen

Submitted: 30 June 2007 / in revised form: 5 December 2007 / Published online: 31 January 2008

Abstract The bent sections from a main steam pipe in a thermal power plant in Shanghai were examined after 165,000 h service at 550 °C under 13.73 MPa pressure. The residual life of the bend sections is determined by evaluation of the service stresses and testing to obtain creep rupture data. Metallographic analysis and tensile, impact, and hardness tests are also conducted. These combined tests show that the properties of the steel deteriorated during service, displaying embrittlement tendencies; the corresponding microstructures exhibit grain boundary weakening and creep damage characteristics. However, considering no evidence of localized damage in the form of creep cavitation or surface cracks was observed in the examined parts, considering the residual life of the bends at service condition, they are adequate for an additional 44,000 h of operation. It is recommended that a health assessment should be taken after 25,000 h service exposure for safety reasons.

Keywords Main steam pipe · Microstructure · Finite element analysis · Residual life assessment

Introduction

Many power plants have been operating for more than 20 years, and the components in these plants have been used at elevated temperatures up to or exceeding the original design life. High-temperature components experience severe service conditions that lead to degradation in the microstructure and properties. Because of this degradation, it is necessary to assess the residual life of exposed components. The creep damage of the materials from components in long-term service has been surveyed to evaluate the residual life. There are few reports about residual life assessment of high-chromium (Cr) ferritic steels; however some investigations of creep damage have focused on hardness measurement, the recovery of lath structure, and coarsening of precipitating carbides [1–3]. The hardness of high-Cr ferritic steels decreases during recovery of the lath structure and coarsening precipitates during creep deformation. Additionally, the lath width and precipitate size increase during accelerated creep. On the contrary, some of the investigations [1] of X20CrMoV12.1 steam pipes that have been in long-term service indicated that the properties degraded severely but no softening occurred. It is believed that the precipitation hardening by fine carbide intralaths as well as stabilization of $M_{23}C_6$ subgrain structure by carbides are decisive factors for the high creep strength of this steel [2].

This paper describes the damage evaluation of the mechanical properties and microstructure as well as residual life assessment for bent pipe sections of a X20CrMoV12.1 main steam pipe in a power plant in Shanghai. The steam pipe has been in service for 23 years, and it has been operating at isothermal and constant pressure condition (550 °C/13.73 MPa) more than 165,000 h. The chemical composition of the X20CrMoV12.1 steel investigated is given in Table 1.

Z.-F. Hu (✉) · G.-Q. He · C.-S. Chen
School of Materials Science and Engineering, Tongji University, Shanghai 200092, China
e-mail: huzhengf@mail.tongji.edu.cn

Z.-G. Yang
Department of Materials Science, Fudan University, Shanghai 200433, China

Table 1 The chemical composition of examined pipe

Composition, wt%									
C	Mn	S	P	Si	Cr	Mo	V	Ni	Cu
0.23	0.64	0.006	0.02	0.36	11.23	1.00	0.32	0.72	0.08

Experiment and Procedures

The test material was cut from three bends at 45° outboard position of a 273 mm outside diameter (OD) by 26 mm thick main steam pipe of X20CrMoV12.1. A sample from a section of virgin pipe in the as-received state was also studied. The mechanical properties were investigated under room temperature and at the service temperature of 550 °C. Tensile tests were conducted using a 100 kN machine operated at constant strain rate. Full-size Charpy V-notch impact specimens were also tested. Hardness measurements were performed at a standardized machine load of 375 kg on testpieces. Tensile tests were carried out on the base metal in both the longitudinal and transverse directions of the main steam pipe. The accelerated stress rupture tests were carried out at 550 °C at various stress levels in the range of 150 to 260 MPa. The variation of the yield strength (0.2% proof stress) and ultimate tensile strength (UTS) with temperature of testing are shown in later tables.

The microstructural investigations were performed using analytical transmission electron microscopy (TEM); the transmission microscopy was carried out on both foil samples and carbon extraction replicas using a PHILIPS CM200 (National Microanalysis Center, Materials Science Department, Fudan University, Shanghai) transmission electron microscope operating at 200 kV. Both the foil and carbon extraction replicas for TEM study were prepared from the pipe samples. The methods of preparing the TEM samples are described in many references [4].

Stress analysis was carried out using finite element analysis software and reflects the stresses under service conditions. The residual life assessment of the main steam pipe is determined from the comprehensive results, including mechanical tests, microstructure investigation, and stress analysis.

Results and Discussion

Mechanical Properties

The mechanical properties of the examined materials tested at room temperature are given in Table 2. The yield strength $\sigma_{0.2}$ and ultimate tensile strength σ_b of exposed samples decrease about 30%, and the toughness is less than 20% of that of the material in the as-received state; however, the hardness shows no significant changes. These results show that the properties of the exposed materials degraded, and the most spectacular change of the mechanical property is the decrease of toughness after long-term service exposure. This means that the base metal of the exposed pipe is much more brittle at room temperature. The same result has been obtained by others [5, 6]. The mechanical properties of the samples tested at high temperature are given in Table 3. The strength as well as toughness of exposed samples decreases slightly, and there is a distinct change in toughness. Toughness of the exposed materials at high temperature is about 30% less compared with the as-received sample tested at the same condition. It is shown that there is an increasing trend of toughness and brittleness transformation temperature with prolonged exposure time at service condition.

Table 2 Mechanical properties of virgin and service-exposed materials at room temperature

Material	SI No. and direction		Tensile strength, MPa		EA (*A*), %	RA (*Z*), %	Toughness (*Akv*), J	Hardness, HB
			$R_{p0.2}$	R_m				
Bend	1	A	575	778	20	44	20	220
		H	556	766	21	44	20	227
	2	A	566	775	20	46	23	230
		H	568	776	20	45	20	232
	3	A	561	774	19	47	21	230
		H	567	777	19	41	21	224
Virgin	1	A	695	777	26	59	113	230
	2	A	702	776	26	59	114	234
	3	A	685	776	24	60	119	229
EN10216-2			>490	690–840	>14		>27	

A, axial; H, hoop

Table 3 Short-time tensile properties of virgin and service-exposed materials at high temperature

Material	SI No. and direction		Tensile strength, MPa		EA (A), %	RA (Z), %	Toughness (Akv), J
			$R_{p0.2}$	R_m			
Bend	1	A	357	444	18	50	109
		H	360	445	20	48	100
	2	A	365	447	18	51	115
		H	358	442	19	54	102
	3	A	378	466	21	73	113
		H	361	441	19	50	101
Virgin	1	A	379	472	24	71	136
	2	A	369	465	22	72	142
	3	A	378	466	21	73	135
EN10216-2			>250				

A, axial; H, hoop

Microstructure

Scanning electron microscopy (SEM) was used to inspect the fracture surfaces of the test samples. Figure 1 (a) shows the fracture surfaces of tensile test from an exposed sample at room temperature. This sample displays almost complete intergranular fracture on a macroscopic level, although the fracture mode is ductile rupture. Subcracks propagate along grain boundaries, and wedge cracks appear at triple points. The fracture facets are quite flat, even though a process of tensile necking had taken place. Such fracture implies a weakness of the grain boundaries, which is caused by the segregation of phosphorus and the presence of coarsened carbides in the grain boundaries during long-term exposed service at high temperature [7]. Figure 1(b) shows the fracture surfaces of tensile test from the same exposed sample tested at 550 °C. It shows that the fracture was transgranular ductile rupture; however, a few subintergranular cracks can be seen in the fracture facets. These observations are consistent with the trend toward weakening of the grain boundaries with exposed time.

The general TEM microstructure of the sample is shown in Fig. 1(c). Obviously, the main structure is a typical tempered martensite containing laths and many coarsened carbide precipitates along grain boundaries. The ferrite regions appear very clean in the TEM image, and most regions contain some finer precipitates. No form of intergranular cavities was observed in the foil sample, but some evidence of creep damage can be seen in TEM. The shapes of the laths are changed; in particular, the lath boundaries look like bamboo knots, called cell structure, which is a typical microstructure morphology caused by creep [8]. Many low dislocation density regions appeared in the lath structure, and some typical substructures can be seen in Fig. 1(d). The substructure seems to develop as subgrains boundaries are formed by dislocation movement during the creep process. A significant reduction of dislocation density is observed, and few dislocation-free regions can be seen.

Extensive carbide precipitates can be seen at prior austenite and martensite lath boundaries, with the finer precipitates in martensitic laths. Large coarsening carbides in irregular spheroid formed along the boundaries. Compared with virgin material, the carbide morphology coarsened distinctly.

The observations indicate that the matrix of the tempered martensite has undergone a deterioration during long-term creep. The dislocations climbed or glided and terminated at boundaries. As the number of dislocations at the boundaries increased, networks formed and substructures developed. The carbides morphology in boundaries coarsened distinctly, and most of the strengthening phase have dissolved or coarsened. However, the tiny V-rich precipitates that formed during service increased the hardness and are responsible for the hardness maintenance in the material [9].

Stress Analysis

In the absence of discernible cavitation and flaws, stress rupture tests were selected to assess the condition of the main pipe. One of the most widely used techniques for life assessment of components involves the removal of samples and conducting accelerated tests at service temperature. An estimate of the residual life is then made by extrapolation of the results to the service conditions.

Table 4 list the results of accelerated test at 550 °C. Stress rupture data have been plotted in term of log stress with rupture time in Fig. 2. The curves show that stresses are linear with rupture times; thus, the threshold strength of the main steam pipe at 550 °C was determined by extrapolation method to be:

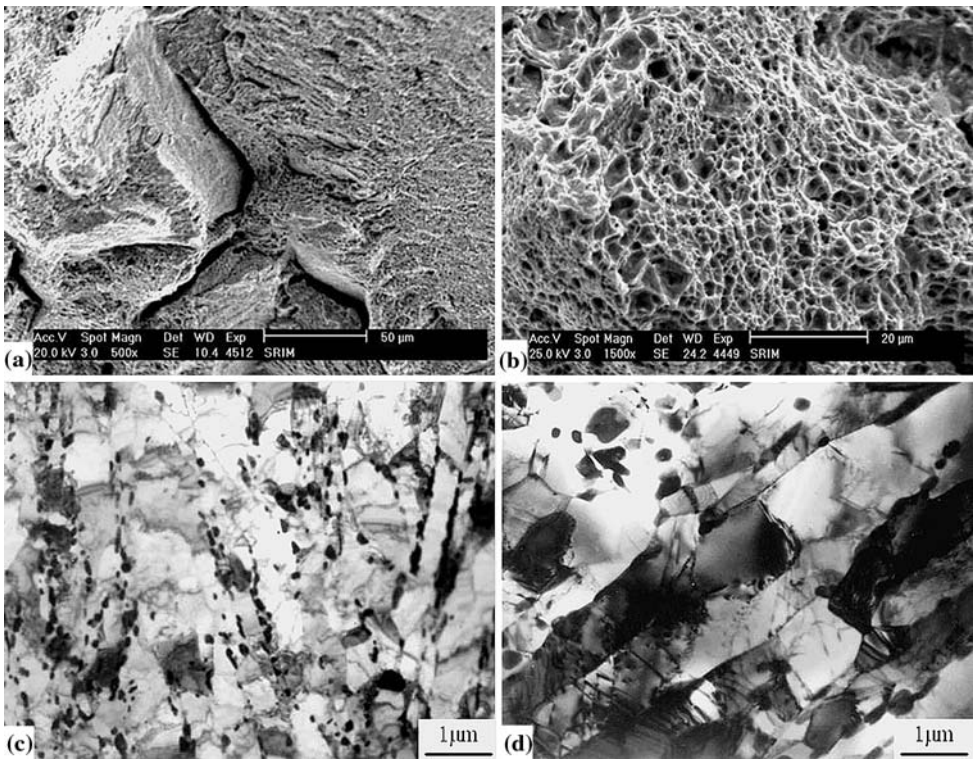

Fig. 1 (**a**) Scanning electron fractographs of exposed sample from tensile test at room Temperature. (**b**) Scanning electron fractographs of exposed sample from tensile test at 550 °C. (**c**) TEM micrograph of thin foil from thin foil from exposed sample. (**d**) TEM micrograph of thin foil from thin foil from exposed sample (magnified)

Table 4 Stress rupture properties of service exposed bend pipe at 550 °C

Sample No.	Stress (σ_s), MPa	Rupture time, h	EL (A), %	EA (Z), %
1	260	17.0	33.1	79.6
2	250	24.5	34.0	79.8
3	220	171.5	35.8	82.0
4	210	366.0	39.6	82.4
5	200	605.0	35.6	82.8
6	190	1190.5	46.5	83.2
7	180	1695.0	35.1	83.4
8	170	3334.0	30.4	82.1
9	160	5346.0	39.4	82.5
10	150[a]	–	–	–

[a] Sample is not ruptured

$$\sigma_{10^5}^{550\,^{\circ}\mathrm{C}} = 131\ \mathrm{MPa} \quad (1)$$

The mechanical tests and rupture data as well as the corresponding microstructure indicate that the properties of the parent metal of exposed bent tube sections show creep damage compared with those of the virgin pipe.

Residual Life Assessment

Standard EN10216-2 [10] gives the creep rupture strength of X20CrMoV12.1 under 550 °C $\sigma_{R,100,000} = 128$ MPa.

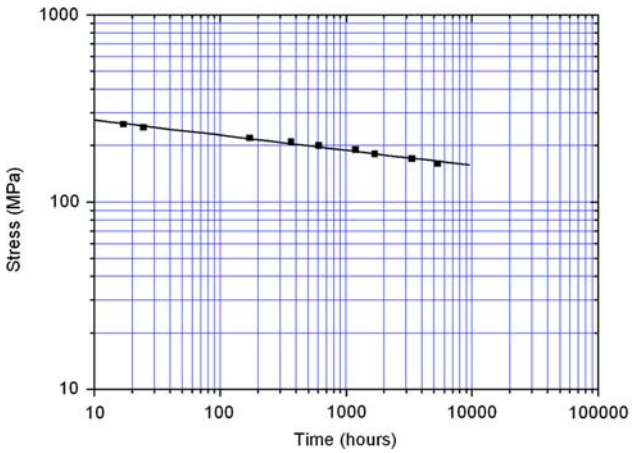

Fig. 2 Plot of stress with rupture time for service exposed bend at 550 °C

This threshold strength of virgin material is less than the strength of the exposed material, $\sigma_{10^5}^{550\,^{\circ}\mathrm{C}} = 131$ MPa, determined by extrapolation from accelerated testing.

Finite-element analysis is used to calculate the stress distribution in a pipe section. The model comprises a pipe bend (90°) to which straight pipes were attached to both ends. Thus numerical influences from boundary conditions on the calculated stresses and strains in the pipe bend could be minimized. The stress analysis takes into account only the internal pressure and ignores all other loads. Further, it was decided to fix one straight pipe end and load an axial

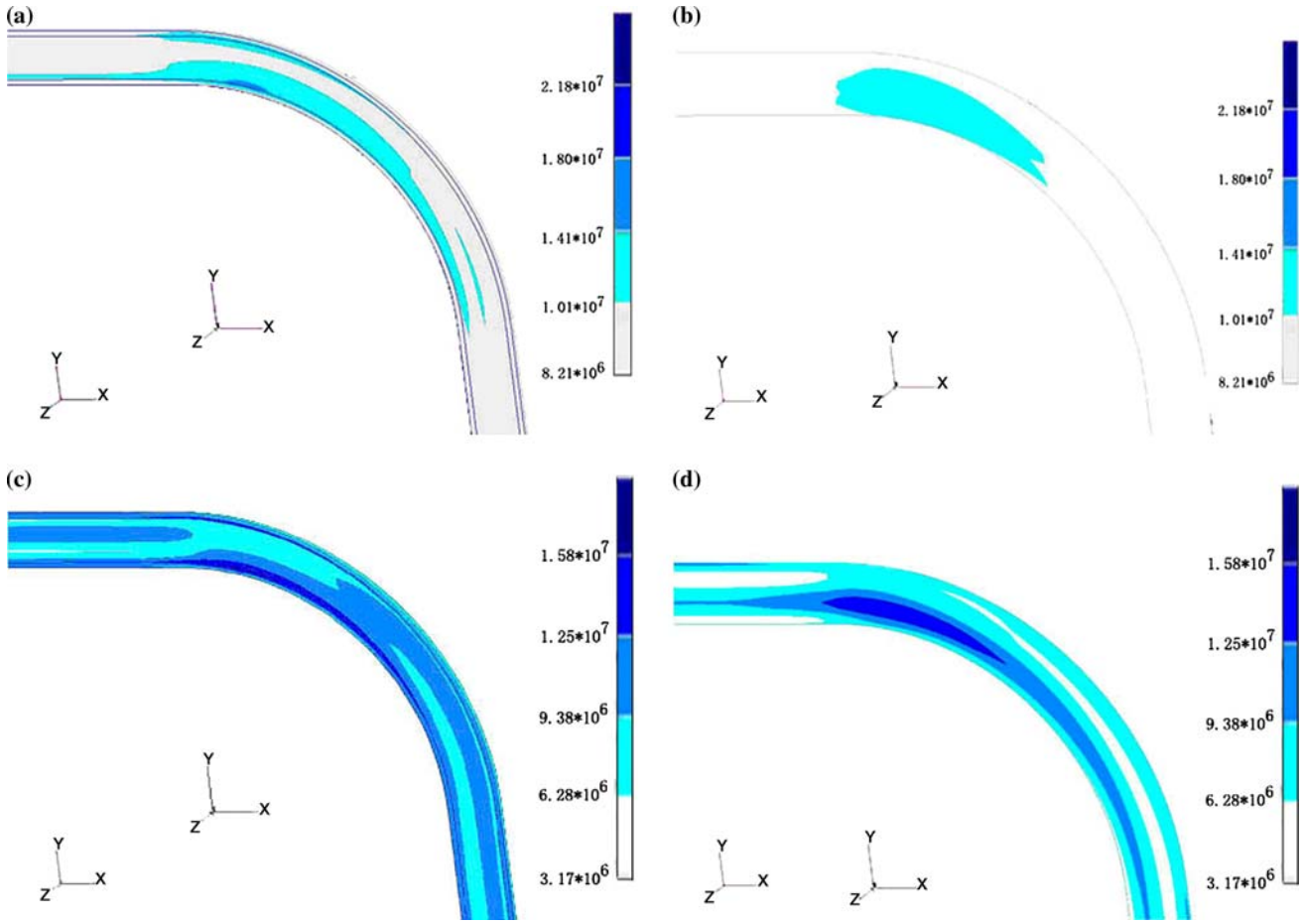

Fig. 3 (**a**) Distribution of the principal stress (internal of bend). (**b**) Distribution of the principal stress (external of bend). (**c**) Distribution of the von Misesl stress (internal of bend). (**d**) Distribution of the von Misesl stress (external of bend)

pressure of $(PD/4t) = 36.4$ MPa on the other end; D and t are the diameter and thickness of the surveyed pipe, respectively. Young's modulus for the material is given as 180,000 MPa (N/mm^2) from tensile test, and Poisson's ratio is assumed to be 0.3. In order to obtain reasonable and accurate results, the analysis of the thick-wall bend attached to straight ends is defined by three-dimensional (3D) cells. To incorporate the actual sizes and space structure of the exposed pipe, the model was set using a geometry model tool in NASTRAN software. The optimized finite element mesh method was employed after the model was established.

Generally, the stress to cause failure may be considered to be either yielding or rupture stress, depending on the criteria used. The corresponding failure theories also consider two types of failure: reaching the ultimate tensile stress for rupture and reaching the Mises yield criterion for yield failure. The calculated results were presented in the form of principal stress (rupture) and Von Mises stress (yielding) simultaneously. The distributions of principal stress are given in Fig. 3(a) and (b). Except for the peak value induced by loading artificially, the principal stress is 101 MPa. The von Mises stress is given in Fig. 3(c) and (d) and displays the peak stress of about 125 MPa. From above results, under actual operating conditions, the maximum resultant stress loading on the pipe is $\sigma_1 = 125$ MPa. This stress was used to evaluate residual life of the bent sections.

With the results of accelerated test and stress analysis, the permitted stress $[\sigma]$ expressed is:

$$[\sigma] = \frac{\sigma_{10^5}^{550\ ^\circ\mathrm{C}}}{n} \tag{2}$$

Here n is safety factor (generally, 1.2–1.65), and we take the value of $n = 1.5$. Therefore, the bent section of the main pipe has permitted stress, from redesign viewpoint of:

$$[\sigma] = 131/1.5 = 87.3 \text{ MPa} \tag{3}$$

Compared with the maximum resultant stress derived from finite element analysis:

$$[\sigma] = 87.3 \text{ MPa} < \sigma_T = 125 \text{ MPa} \tag{4}$$

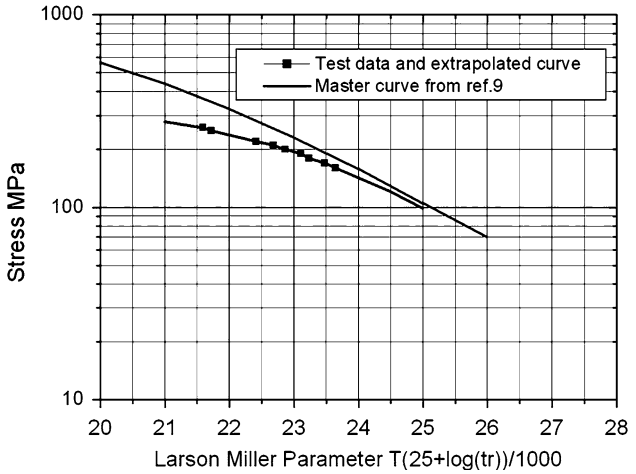

Fig. 4 Plot of stress vs Larson Miller parameter (LMP) for parent metal of bend

Equation 8 means, from the redesign viewpoint, that the exposed pipe could not meet the safety criteria for operation for 100,000 h after 23 years service.

The rupture data for the specimens have been plotted in terms of log (stress) versus Larson-Miller parameter in Fig. 4, where LMP is expressed:

$$\mathrm{LMP} = T(25 + \log t_r) \tag{5}$$

where T is the absolute temperature in K, and t_r is the rupture time in hours.

Analysis of rupture data indicates that the properties of the exposed steel are comparable to those of the master curve of virgin pipe [11], suggesting no appreciable creep damage. The test data points of the stress versus LMP plot for the service-exposed material are fairly close to the master curve for virgin material when the stress is less than 200 MPa. The master curve for the virgin material has been extrapolated to a lower stress value that is below the operating hoop stress ($\sigma_h = PD/2t = 72.1$ MPa) of the service-exposed main steam pipe. The remaining life of the service-exposed main steam pipe predicted at 72.1 MPa and at 550 °C is shown in Fig. 4. At the operating hoop stress of 72.1 MPa for the service-exposed pipes, the LMP value as read from the graph is about 25,730. At this value of LMP, one would expect a very long life. As is customary, an inspection life of straight pipe after >100,000 h is recommended. However, considering that the maximum resultant stress on the bent section is $\sigma_1 = 125$ MPa, the LMP value as read from the graph is about 24,398 and the expected residual life is about 44,200 h. The results for the parent metal in the bent section predict a remaining life of about 44,200 h at most highly stressed locations, although failure of the straight sections should not occur in 100,000 h of operation.

This analysis thus suggests that the remaining life at 550 °C is a minimum of 44,200 h for the service, provided there is no evidence of localized damage in the form of surface cracks or cavitation. Additionally, it is recommended that another health check of the expected service of the exposed bent sections be carried out after 22,000 h of service. During shutdown of the plant, nondestructive tests, namely, dimensional (thickness and diameter) measurement, and in situ metallography may be carried out to assess the condition of the materials for their future serviceability.

Conclusions

An increasing trend of brittleness of the parent metal of X20CrMoV12.1 is seen with prolonged exposure at service conditions. Corresponding microstructural investigations show that carbide coarsening and martensite structure deterioration also occur during long-term exposure service at 550 °C. The residual life of bent sections of main pipe of X20CrMoV12.1 is about 44,000 h, provided there is no evidence of localized damage in the form of surface cracks or cavitation. Even though the straight sections of the main steam pipe appear to be in a reasonably good state of health, it is recommended that another health check be carried out after 22,000 h of additional service. Additionally, during shutdown of the plant, nondestructive tests (NDT), namely, dimensional (thickness and diameter) measurement, hardness measurement, and in situ metallography should be carried out to assess the condition of the materials for their future serviceability.

Acknowledgments This work was supported by the National Natural Science Foundation of China under contract no. 50771073 and National Basic Research Program of China under contract no. 2007CB714705.

References

1. Masuyama, F., Nishimura, N., Sasada, A.: CAMP-ISIJ, **11**, 614 (1998).
2. Ennis, J.P.: Creep strengthening mechanisms in high chromium steels. In: Bakker, W.T., Parker, J.D. (editors). Proceedings of the Third Conference on Advances in Materials. Technology for Fossil Power Plants. London (UK): The Institute of Materials, pp. 187–194 (2001).
3. Sawada, K., Maruyama, K., Hasegawa, Y., Muraki, T.: Creep life assessment of high chromium ferritic steels by recovery of martensitic lath structure. Proceedings of Eighth International Conf. on Creep and Fracture of Engineering Materials and Structures, Tsukuba, Japan, Nov. 1–5, 1999.
4. Hu, Z.F., Wu, X.F., Wang, C.X.: HRTEM study on precipitates in high CoNi steel. J. Mater. Sci. & Tech. **20**, 425/528 (2004).
5. Vodarek, V., Strang, A.: Effect of nickel on the precipitation processes in 12CrMoV steels during creep at 550 °C. Scr. Mater. **38**, 101 (1998).
6. Ennis, P.J., Zielinska-Lipiec, A., Filemonowicz, A.: Quantitative comparison of the microstructure of high chromium steels for

advanced power stations. In: Strang, A., Cawley, J., Greenwoof, G.W. (editors): Microstructure of High Temperature Materials, No. 2, The Institute of Materials, London, U.K., pp. 135–143 (1998).
7. Hu, Z.F., Yang, Z.G.: An investigation of the embrittlement in X20CrMoV12.1 power plant steel after long-term service exposure at elevated temperature. Mater. Sci. Eng. A, **383**, 224–228 (2004).
8. Chan, R.W., Haasen, P.: Physical Metallurgy, part 2 [M], North-Holland Physics Publishing, Netherlands (1983).
9. Hu, Z.F., Yang, Z.G.: Identification of the precipitates by TEM and EDS in X20CrMoV12.1 for long-term service at elevated temperature. J. Mater. Eng. Perform. **12**(1), 106–111 (2003).
10. European Standard: EN10216-2, Seamless steel tubes for pressure purpose—Technical delivery conditions, Part 2: Non alloy and alloy steel tubes with specified elevated temperature properties.
11. Weber, J., Klenk, A., Rieke, M.A.: new method of strength calculation and lifetime prediction of pipe bends operating in the creep range. Int. J. Pressure Vessels Piping **82**, 77–84 (2005).